A Cambrian crown annelid reconciles phylogenomics and the fossil record

Hong Chen[1,2,3*], Luke A. Parry[4,5*], Jakob Vinther[6,7], Dayou Zhai[1,2], Xianguang Hou[1,2], Xiaoya Ma[1,2,8**]**

[1]Yunnan Key Laboratory for Palaeobiology, Yunnan University, Kunming 650500, Yunnan Province, China
[2]MEC International Joint Laboratory for Palaeobiology and Palaeoenvironment, Yunnan University, Kunming 650500, Yunnan Province, China
[3]School of Biological Sciences and Technology, Liupanshui Normal University, Liupanshui 553004, Guizhou Province, China
[4]Department of Geology and Geophysics, Yale University, 210 Whitney Avenue, New Haven, CT, 06511, USA
[5]Department of Earth Sciences, University of Oxford, South Parks Road, Oxford, OX1 3AN, UK
[6]School of Earth Sciences, University of Bristol, Wills Memorial Building, Queens Road, Bristol BS8 1RJ, UK
[7]School of Biological Sciences, University of Bristol, Life Sciences Building, 24 Tyndall Avenue, Bristol BS8 1TQ, UK
[8]Centre for Ecology & Conservation, University of Exeter, Penryn Campus, Cornwall TR10 9TA, UK

* These authors contributed equally to this work
**e-mail: x.ma2@exeter.ac.uk and xghou@ynu.edu.cn

Annelids are among the most disparate animal phyla, encompassing ambush predators, suspension feeders and terrestrial earthworms[1]. Early annelid evolution remains obscure or controversial[2,3], partly due to discordance between molecular phylogenies and fossils[2,4]. Cambrian annelid fossils have morphologies indicating epibenthic lifestyles, whereas phylogenomics recovers sessile, infaunal and tubicolous taxa as an early diverging grade[5]. Magelonidae and Oweniidae (Palaeoannelida[1]) are the sister group of all other annelids but contrast with Cambrian taxa in both lifestyle and gross morphology[2,6]. We describe a new fossil polychaete, *Dannychaeta tucolus*, from the early Cambrian Canglangpu Formation[7], preserved within delicate, originally organic dwelling tubes. The head has a well-defined spade-shaped prostomium with elongate ventrolateral palps. The body has a wide, stout thorax and elongate abdomen with biramous parapodia with parapodial lamellae. This character combination is shared with extant Magelonidae, and phylogenetic analyses recover *Dannychaeta* within Palaeoannelida. *Dannychaeta* is the oldest polychaete unambiguously belonging inside

crown annelids, providing a constraint on the tempo of annelid evolution and revealing unrecognised ecological and morphological diversity in ancient annelids.

Systematic Palaeontology

Phylum: Annelida Lamarck, 1809
Unranked: Palaeoannelida Weigert & Bleidorn, 2016
Family: Magelonidae Cunningham & Ramage, 1888
Dannychaeta tucolus gen. et sp. nov.

Etymology: *Danny:* referring to Danny Eibye-Jacobsen, for his contributions to our understanding of early annelids; *chaeta* (Latin): bristle; *colus* (Latin): dwelling in; *tubus* (Latin): tube.

Holotype: YKLP 11382 part and counterpart (Fig. 1, Extended Data Fig. 1)

Referred material: YKLP 11383—11402 (Fig. 2-3, Extended Data Figs. 2-6).

Locality and Horizon: Canglangpu Formation, Cambrian Stage 3, Hongjingshao Member (~514 Ma), at southwest of Guanshan reservoir, Chenggong, Kunming, China[7].

Diagnosis for genus: Elongate, slender polychaetes with organic dwelling tubes. Head with anteriorly tapering spade-shaped prostomium, with paired palps attached ventrolaterally near the mouth. Body heteronomously segmented, with wider thorax containing at least 8 chaetigers. Parapodia with lateral lamellae in the posterior part of the abdomen. Abdominal parapodia biramous, unknown in thorax. Capillary chaetae in both rami, occurring in tight parallel bundles.

Description: The holotype (Fig. 1, Extended Data Fig. 1) is incomplete posteriorly (~40 mm long), showing the wider anterior region (thorax; max width 3.9 mm) (Fig. 1a-e) and abdomen (~1.9 mm exclusive of parapodia) (Fig. 1h-i). The number of thoracic segments would consist of ≥8 chaetigers, extrapolating from segment spacing (15.5 mm length and 1 segment per 1.9 mm). The prostomium is a spade-shaped lobe (Figs 1c-e, 2a-h, Extended Data Figs. 1a-g, 2a-h) and is longer (~4 mm) than wide (~2 mm). The relief of overlapping anatomical features preserved on different planes indicates that the prostomium is dorsal of the palps (Fig. 1d-f, 2b-d). The palps cross over each other in the holotype (Fig. 1d-f), are incompletely preserved anteriorly, but are ≥30% the length of the thorax. A specimen in ventral view shows palps inserting ventrolaterally, anterior of a putative burrowing organ (Fig. 2a-d). The prostomium has a faint pair of tapering ridges (Fig. 2d). The gut is preserved as a carbonaceous film (Fig. 3f) that terminates adjacent to palp bases (Fig. 1d-f), indicating palp attachment near the mouth opening.

Abdominal parapodia are distinct lobes, projecting ~300 μm from the body (Fig. 3c-e). Anterior abdominal chaetae in the holotype are ~500 μm long (Fig. 1h). In narrower midbody fragments, chaetae are ~800 μm long (e.g. Fig. 3d), suggesting variable chaetation along the body. Abdominal chaetae are in tight fascicles (Figs 1j, 3c-e, Extended Data Fig. 3k) and are most clear using fluorescence microscopy (Fig. 3d). The chaetae are directed slightly anteriorly (Fig. 1i) which is used to orient fragmentary specimens. In two specimens, lateral lamellae occur adjacent to chaetal bundles (Fig. 3g). Lamellae are crescent-shaped and approximately half the body width in length, with a dorsolateral (Extended Data Fig. 1k) to dorsal (Extended Data Fig. 5f-h) placement. As the rami are often parallel, biramous morphology is revealed by subparallel chaetal bundles (Fig. 3d) or rare oblique views (Fig. 3h, Extended Data Fig. 5). Fine details of chaetal morphology are obscure but are consistent with capillaries in the abdomen (e.g. Fig. 3d).

The pygidium is never well-preserved, but one specimen has putative pygidial cirri (Extended Data Fig. 5j, k). An ovoid structure between chaetiger one and three is of uncertain identity but resembles a blood lacuna (Fig. 1d-f, Extended Data Figs. 1h-j, 4g).

Eight specimens are preserved within a structure that extends beyond the body margin and chaetae (Fig. 3a-f, i-k, Extended Data Figs. 2-4). This is parallel to the body axis, approximately four times the body width (excluding parapodia) (Fig. 3a) with a sharp boundary with the matrix, which is visible using light (Fig. 2f) and fluorescence (Fig. 3h) microscopy and elemental maps for iron (Extended data Fig. 3f). This structure is consistent with a dwelling tube, or tube-lined burrow. The tube has a slightly darker appearance relative to the matrix and lacks identifiable agglutinated bioclasts or grains. Tubes have slight relief (Extended Data Fig. 3g) and sometimes have thick walls at their margins (Extended Data Fig. 5c-e), due to compaction. Like the body, the tube contains iron (Fig. 3f) localised to small grains in the matrix that appear bright in SEM backscatter images (Extended Data Fig. 3f). This is consistent with an organic composition, with organic material acting as a substrate for pyrite formation[8]. Specimens preserved in tubes vary from well-preserved with delineated parapodia/chaetae

(Fig. 3c-e, Extended Data Fig. 3) to highly effaced, indicating in situ decay[9] (Extended Data Fig. 4,6). Preservation quality varies along individual specimens (e.g. Extended Data Figs. 3a-d).

Discussion

Due to low preservation potential[9], annelid body fossils are rare and distributed discontinuously and unevenly through geological time[10]. Diverse fossil polychaetes are known from the early and middle Cambrian deposits (e.g. Sirius Passet[3,11] and Burgess Shale[12]), but rare from China[13,14]. Cambrian annelids typically are generalised polychaetes in morphology, with well-developed biramous parapodia (suggesting motility[15]), elongate chaetae and a pair of palps[2,3,6,11]. They cannot be assigned to extant annelid subclades[6,12] and lack proposed annelid synapomorphies (e.g. the prostomium-peristomium head structure[3] and typically pygidial cirri[12]) and are interpreted as stem-group annelids[6]. The lack of Cambrian crown annelids has prompted hypotheses of relatively late crown group diversification, perhaps late Cambrian/Ordovician[4], when jawed polychaetes become diverse and abundant[16].

Both molecular[1,5,17] and morphological[18] phylogenies have converged on scenarios where annelids evolved from polychaete-like ancestors. However, reconciling fossil and phylogenomic evidence has been challenging[2,6,12,15]. Molecular phylogenies recover a grade of infaunal, sessile and tube-dwelling taxa as deep branches[1,5], including Magelonidae, Oweniidae, Chaetopteriformia and Sipuncula. These groups differ from Cambrian polychaetes in terms of gross morphology and inferred mode of life[6]. A tube-dwelling annelid ancestor has been proposed[19] (although see[20]), which is contradicted by interpretations of the fossil record[15], and morphological hypotheses regarding the origin of annelid body plan features, e.g. segmentation and parapodia[18,20]. Fossil specimens interpreted as sipunculans (which phylogenomic studies recover within Annelida[1,5]) are known from the early Cambrian Chengjiang Lagerstätte[21] but are rare and poorly known. If correctly interpreted, the oldest fossil crown annelids therefore belong to taxa that have lost most annelid synapomorphies[6], including segmentation[22]. Magelonidae and Oweniidae (Palaeoannelida[1]) are recovered as the sister group of all other annelids and so have featured prominently in recent discussions of the annelid ancestor[15,17,19]. These families are unusual among polychaetes, as they lack nuchal organs, possess monociliated epidermal cells and simple nervous systems[1,17].

Dannychaeta is dissimilar in gross morphology to that of previously known Cambrian polychaetes, but shares derived characters with extant Magelonidae. A spade-shaped prostomium with ventrolateral palps (Fig. 2) is characteristic for Magelonidae, which also have a differentiated thorax composed of eight or nine chaetigers[23,24]. Other well-known Cambrian annelids lack a clearly demarcated head and prostomial lobe[3] (but have lateral palps[15]), suggesting the typical annelid head structure evolved after the origin of a segmented body, parapodia and palps[3]. The presence of a differentiated head in *Dannychaeta* is unique among Cambrian annelid fossils, indicating in itself a phylogenetic position proximal to or within the annelid crown group[3]. The significance of the putative blood lacuna is uncertain, but small ring shaped vessels occur in *Magelona*[23] and a larger lacuna occurs in *Poecilochaetus*[25]. However, both are placed more anteriorly, nearer the prostomium.

Although not widespread (~7% of species[24]), several magelonid species live in tube-lined burrows[26] with an organic/parchment-like composition, some adhered sediment grains/bioclasts. These tubes are similar in inferred construction materials and dimensions relative to the body as in *Dannychaeta*. The presence of both obliquely and parallelly oriented specimens (e.g. Extended Data Figs. 2, 4) suggests at least some transport prior to burial.

We reconstruct *Dannychaeta* as a sessile, infaunal polychaete that fed in the water column using elongate palps (as in extant Magelonidae[24,26]; Fig. 4a, b). Our phylogenetic analyses recover *Dannychaeta* in the magelonid stem group (Fig. 4c, Extended Data Figs. 6, 7). Parapodial and chaetal morphology differ in some details in *Dannychaeta* and Magelonidae. In extant *Magelona,* the chaetae of the abdomen are hooded hooks, which are generally shorter than the thoracic capillary chaetae and occur in rows[24], whereas abdominal chaetae in *Dannychaeta* resemble capillaries held in bundles (Fig. 3c-e). Hooded hooks in certain families share details of ultrastructure and formation[27] resulting in a proposed close relationship between Capitellidae, Spionidae and Magelonidae[27], which is not supported by phylogenomics[1]. The absence of hooded hooks in *Dannychaeta* may therefore provide consilient evidence of convergent chaetal evolution in these families. Parapodial lamellae also differ in some details in *Dannychaeta,* as they are dorsolaterally placed, but occur partially in inter-ramal space in some species in *Magelona*[24]. *Dannychaeta* is larger than extant magelonids that are typically less than 1 mm wide[24], although tubicolous species (e.g. *M. alleni*) achieve the largest widths and share a more robust anterior region (thorax) with *Dannychaeta*[24].

Other non-pleistoannelid polychaetes also share some characters with *Dannychaeta. Spiochaetopterus* has elongate palps, a differentiated anterior region and organic tubes[28]. However, chaetopterids have ridge-like parapodia (tori) with short, hooked chaetae (uncini[2]), which are distinct from laterally projecting, lobate parapodia in *Dannychaeta.* The head of *Spiochaetopterus* is neither a distinct anterior lobe nor spade shaped. Nevertheless, chaetopterids branch proximally to Palaeoannelida[5]. A close relationship between *Dannychaeta* and chaetopterids would also suggest the presence of tubicolous, early branching crown group annelids in the early Cambrian.

Annelid tube fossils are well-documented[10]. Some late Ediacaran and early Cambrian fossil tubes are tentatively assigned to annelids or described as of 'annelid grade'[30], but lack diagnostic features that would allow confident phylogenetic placement. Tube dwelling has evolved several times among extant annelids, and 'annelid mimicking' taxa with lophophorate affinities are well known from the early Palaeozoic[29], indicating caution should be exercised when assigning fossil tubes. The controversial late Ediacaran tubular fossil *Cloudina* has been tentatively reconstructed as an annelid based on the presence of a tubular gut[30].

Regardless of the phylogenetic position and fossil record of sipunculans[4,21,22], *Dannychaeta* confirms crown annelids as minimally early Cambrian in age, revealing early exploration of sessile ecological niches, over a hundred million years prior to other unambiguous examples of tubicolous annelids[10,29]. *Dannychaeta* reveals that stem-group annelids coexisted with members of the crown group in the early Cambrian and exhibited a diversity of life modes, including epibenthic[15] and sessile forms.

1 Weigert, A. & Bleidorn, C. Current status of annelid phylogeny. *Organisms Diversity & Evolution*, 1-18 (2016).

2 Eibye-Jacobsen, D. & Vinther, J. Reconstructing the ancestral annelid. *Journal of Zoological Systematics and Evolutionary Research* **50**, 85-87, doi:10.1111/j.1439-0469.2011.00651.x (2012).

3 Parry, L., Vinther, J. & Edgecombe, G. D. Cambrian stem-group annelids and a metameric origin of the annelid head. *Biology Letters* **11**, 20150763 (2015).

4 Sperling, E. A. *et al.* MicroRNAs Resolve an Apparent Conflict Between Annelid Systematics and Their Fossil Record. *Integrative and Comparative Biology* **276**, 4315-4322 (2009).

5 Weigert, A. *et al.* Illuminating the base of the annelid tree using transcriptomics. *Molecular Biology and Evolution* **31**, 1391-1401 (2014).

6 Parry, L. A., Edgecombe, G. D., Eibye-Jacobsen, D. & Vinther, J. The impact of fossil data on annelid phylogeny inferred from discrete morphological characters. *Proceedings of the Royal Society B* **283**, 20161378 (2016).

7 Zeng, H., Zhao, F., Yin, Z., Li, G. & Zhu, M. A Chengjiang-type fossil assemblage from the Hongjingshao Formation (Cambrian Stage 3) at Chenggong, Kunming, Yunnan. *Chinese science bulletin* **59**, 3169-3175 (2014).

8 Gabbott, S. E., Xian-Guang, H., Norry, M. J. & Siveter, D. J. Preservation of Early Cambrian animals of the Chengjiang biota. *Geology* **32**, 901-904 (2004).

9 Briggs, D. E. G. & Kear, A. J. Decay and preservation of polychaetes; taphonomic thresholds in soft-bodied organisms. *Paleobiology* **19**, 107-135 (1993).

10 Parry, L. A., Eriksson, M. & Vinther, J. in *Handbook of Zoology : Annelida - Volume 1: Annelida Basal Groups and Pleistoannelida, Sedentaria I - Annelida - Volume 1:*

Annelida Basal Groups and Pleistoannelida, Sedentaria I (eds Günter Purschke, Markus Böggemann, & Wilfried Westheide) 69-88 (De Gruyter, 2019).

11 Vinther, J., Eibye-Jacobsen, D. & Harper, D. A. An Early Cambrian stem polychaete with pygidial cirri. *Biol Lett* **7**, 929-932, doi:10.1098/rsbl.2011.0592 (2011).

12 Eibye-Jacobsen, D. A reevaluation of *Wiwaxia* and the polychaetes of the Burgess Shale. *Lethaia* **37**, 317-335, doi:10.1080/00241160410002027 (2004).

13 Liu, J. *et al.* Lower Cambrian polychaete from China sheds light on early annelid evolution. *The Science of Nature* **102**, 1-7 (2015).

14 Han, J., Morris, S. C., Cuthill, J. F. H. & Shu, D. Sclerite-bearing annelids from the lower Cambrian of South China. *Scientific Reports* **9**, 4955 (2019).

15 Parry, L. & Caron, J.-B. *Canadia spinosa* and the early evolution of the annelid nervous system. *Science advances* **5**, eaax5858 (2019).

16 Parry, L. A., Edgecombe, G. D., Sykes, D. & Vinther, J. Jaw elements in Plumulites bengtsoni confirm that machaeridians are extinct armoured scaleworms. *Proceedings of the Royal Society B* **286**, 20191247 (2019).

17 Helm, C. *et al.* Convergent evolution of the ladder-like ventral nerve cord in Annelida. *Frontiers in zoology* **15**, 36 (2018).

18 Westheide, W. The direction of evolution within the Polychaeta. *Journal of Natural History* **31**, 1-15, doi:10.1080/00222939700770011 (1997).

19 Beckers, P. *et al.* The central nervous system of Oweniidae (Annelida) and its implications for the structure of the ancestral annelid brain. *Frontiers in Zoology* **16**, 6 (2019).

20 Struck, T. Direction of evolution within Annelida and the definition of Pleistoannelida. *Journal of Zoological Systematics and Evolutionary Research* **49**, 340-345, doi:10.1111/j.1439-0469.2011.00640.x (2011).

21 Huang, D. Y., Chen, J. Y., Vannier, J. & Salinas, J. I. S. Early Cambrian sipunculan worms from southwest China. *Proceedings of the Royal Society B-Biological Sciences* **271**, 1671-1676, doi:10.1098/rspb.2004.2774 (2004).

22 Carrillo‐Baltodano, A. M., Boyle, M. J., Rice, M. E. & Meyer, N. P. Developmental architecture of the nervous system in Themiste lageniformis (Sipuncula): New evidence from confocal laser scanning microscopy and gene expression. *Journal of morphology* (2019).

23 Jones, M. L. On the morphology, feeding, and behavior of *Magelona sp. The Biological Bulletin* **134**, 272-297 (1968).

24 Mortimer, K. in *Handbook of Zoology* (eds W Westheide & G Purschke) (De Gruyter, 2019).

25 Allen, E. The anatomy of *Poecilochaetus*, Claparede. *Quarterly Journal of Microscopical Science* **48**, 79 (1904).

26 Mills, K. & Mortimer, K. Observations on the tubicolous annelid *Magelona alleni* (Magelonidae), with discussions on the relationship between morphology and behaviour of European magelonids. *Journal of the Marine Biological Association of the United Kingdom*, 1-13 (2018).

27 Hausen, H. Chaetae and chaetogenesis in polychaetes (Annelida). *Hydrobiologia* **535**, 37-52 (2005).

28 Barnes, R. D. Tube-building and feeding in the chaetopterid polychaete, Spiochaetopterus oculatus. *The Biological Bulletin* **127**, 397-412 (1964).

29 Ippolitov, A., Vinn, O., Kupriyanova, E. & Jäger, M. Vol. 71 (*Memoirs of Museum Victoria*, 2014).

30 Schiffbauer, J. D. *et al.* Discovery of bilaterian-type through-guts in cloudinomorphs from the terminal Ediacaran Period. *Nature Communications* **11**, 1-12 (2020).

Acknowledgements.

This work was supported by NSFC grant 41861134032, and Yunnan Provincial grants 2015HC029, 2018FA025 and 2018IA073. LAP was supported by a YIBS Donolley Postdoctoral Fellowship. DYZ is supported by the Key Research Program of the Institute of Geology & Geophysics, Chinese Academy of Sciences (IGGCAS-201905). XYM is supported by a Natural Environment Research Council Independent Research Fellowship (NE/L011751/1). We thank Kunhong Chen and colleagues from the Xiazhuang subdistrict office in Chenggong for generous support in field collection. Thanks to Peiyun Cong, Di Wu, Ting Zhao, Yang Zhao and Mengying Yin for help in fieldwork, to Xiaoyu Yang and Huijuan Mai for SEM-EDX technical support, to Runqing Zhou for micro-CT scanning. We thank Danny Eibye-Jacobsen for providing detailed comments on an earlier version of this manuscript and for his continued support and valuable mentorship. We thank Robert Nicholls for the artistic reconstruction of *Dannychaeta tucolus*.

Figure 1 | *Dannychaeta tucolus,* holotype specimen YKLP 11382. a, b, part and counterpart, direct light. **c,** interpretative drawing of counterpart, colour scheme detailed in **f. d,** anterior region of part. **e,** anterior region of counterpart under fluorescent light. Specimen mirrored for easier comparison with part. **f**, interpretative drawing of the anterior, based on both part and counterpart. **g,** Fe map from SEM-EDX analysis. **h**, **i,** abdominal region, counterpart, direct light (h), fluorescent light (i). **j,** close-up of parapodium and chaetae**.** Abbreviations: ch – chaetae, gu – gut, mo – mouth, pl – palp, pa1 – parapodium of segment one, pa8/9 – parapodium of segment eight or nine, pa – parapodium.

Figure 2 | *Dannychaeta tucolus*, anterior region. a, YKLP 11390b, anterior fragment with head and palps. **b,** anterior region of YKLP 11390b, low angle illumination from the northwest. **c,** region as in **b,** fluorescent light. **d,** interpretative drawing outlining anatomical features (colour scheme as in Fig. 1f). **e,** YKLP 11393b specimen preserving anterior region, dwelling tubes and a partial abdomen. **f**, YKLP 11393a, part. **g,** YKLP 11393b, details of anterior region, white arrowheads indicate tube margins. **h,** interpretative drawing of **g.** Abbreviations: pl – palps, pa – parapodium, pro- prostomium, bo – burrowing organ, rd – prostomial ridge.

Figure 3 | *Dannychaeta tucolus*, morphological details. a-f, YKLP 11383. **a,** abdominal region within dwelling tube **b**, interpretative drawing of **a** (colours as in Fig 1). Anteriorly, black filled arrowheads indicate the body margin and white filled arrowheads indicate the tube edge. **c,** close up showing the segmented body and parapodia. **d,** close up of chaetal fascicle. **e,** interpretative drawing outlining chaetal fascicles**. f** close up and SEM-EDX maps. **g-h,** YKLP 11389. **g**, close up showing parapodia and lateral lamellae. **h,** close up of YKLP 11384a showing biramous parapodia, chaetae (white arrowhead indicates tube edge). Abbreviations: ch – chaetae, gu – gut, pa – parapodium, plm – parapodial lamella.

Figure 4 | Reconstruction of *Dannychaeta.* a, technical drawing showing proportions, body regions and gross anatomy, colour scheme is as in Fig 1f, dorsal view (left) and right lateral view (right). Parapodia in the thorax not observed but inferred shown in grey. **b,** life reconstruction showing *Dannychaeta tucolus* living in buried tubes, artwork by Bob Nicholls. **c**, Bayesian phylogenic analysis (365 characters, 143 taxa, mki + gamma model) incorporating *Dannychaeta tucolus*. Numbers at nodes are posterior probabilities with scalebar in number of substitutions per site (see Extended Data figure 7 + 8 for full results and additional information).

Methods

The specimens were studied, photographed at the Yunnan Key Laboratory for Palaeobiology, Yunnan University (YKLP) and at the University of Exeter, and are deposited in YKLP. Photographs were taken using a Canon EOS 5DSR coupled with a MACRO 100 mm lens, and a Leica DFC7000T linked to a Leica M205 FA fluorescent microscope. The excitation wavelength of GFPL is 480 nm, and the excitation wavelength of RFPL is 546 nm. Images used a gain value of 3.3, saturation value of 52.00, gamma value of 0.92. The external light source of the fluorescence microscope was a LEICA KL 300 LED, used for taking white light images. Scanning electron microscope images were collected using a FEI Quanta 650 FEG using an accelerating voltage of 25kv and a working distance of 12.4 mm. Energy dispersive X-ray (EDX) analyses used an EDAX Pegasus using accelerating voltages of 25-30kv with a working distance of 12.4-13 mm.

Phylogenetic analyses were based on a previously published character matrix for annelids and their close relatives[6] which has been updated successively with the addition of new taxa and fossil data[14-16,31]. We performed Bayesian analyses using MrBayes 3.2.6 using the mki model with the Lewis correction for the scoring only of informative characters[32], with default priors for all parameters (ie.g.e. all trees given equal prior probability). Bayesian analyses with and without topological constraints based on phylogenomic trees were used to investigate if the conflicting topologies recovered from morphological and molecular data impacted the phylogenetic position of *Dannychaeta tucolus*. These constraints were constructed by incorporating results from the most recent[17] and taxon rich[33,34] phylogenomic analyses of annelids and are outlined in detail in the supporting information. We followed ref[15] by excluding *Arkonips* and *Guanshanchaeta* from the character matrix as they contain redundant character scores. For both analyses 100 million generations were requested, with the analysis stopping once the average deviation of split frequencies dropped below 0.01. Convergence was then assessed using ESS (>200) and PSRF (~1.0) values for all model parameters. Parsimony analyses without topological constraints were conducted in TNT 1.5[35] (courtesy of the Willi Hennig Society), using both equal weights and implied weights with k=10. Bremer support and jackknife and bootstrap frequencies from 1000 replications were inferred for equal weights trees and frequency differences were inferred from 1000 replicates of symmetric resampling for the implied weights trees.

References

31 Nanglu, K. & Caron, J.-B. A new Burgess Shale polychaete and the origin of the annelid head revisited. *Current Biology* **28**, 319-326. e311 (2018).

32 Lewis, P. O. A likelihood approach to estimating phylogeny from discrete morphological character data. *Systematic Biology* **50**, 913-925 (2001).

33 Struck, T. H. *et al.* The evolution of annelids reveals two adaptive routes to the interstitial realm. *Current Biology* **25**, 1993-1999 (2015).

34 Andrade, S. C. *et al.* Articulating "archiannelids": Phylogenomics and annelid relationships, with emphasis on meiofaunal taxa. *Molecular biology and evolution*, msv157 (2015).

35 Goloboff, P. A., Farris, J. S. & Nixon, K. C. TNT, a free program for phylogenetic analysis. *Cladistics* **24**, 774-786 (2008).

Author contributions

LAP, HC, JV and XYM designed the study and interpreted the fossil specimens and their anatomy. HC, DYZ and XGH collected the specimens. HC prepared and photographed all specimens and performed the EDAX elemental analysis. LAP made the figures, performed the phylogenetic analyses and composed the first draft of the manuscript with substantial input from all co-authors.

Corresponding authors

Correspondance should be addressed to Xiaoya Ma (x.ma2@exeter.ac.uk) or Xianguang Hou (xghou@ynu.edu.cn).

ETHICS DECLARATIONS

Competing interests.

The authors declare no competing interests.

DATA AND CODE AVAILABILITY STATEMENT

All data analysed in this paper are available as part of the published paper, the extended data or supplementary information. The phylogenetic dataset and commands and topological constraints necessary to run the MrBayes analyses are included as NEXUS formatted files. The nomenclatural acts in this publication have been registered at ZooBank (LSID: urn:lsid:zoobank.org:pub:5BC89E47-2955-4539-94FD-D400E8C947FB).

Extended Data Figure Captions

Extended data Figure 1 | Additional details of holotype specimen. a, YKLP 11382a entire specimen, including possible posterior region. **b,** possible posterior region from region shown in **a. c,** YKLP 11382a, box indicates region used for fluorescence microscopy. **d,** interpretative drawing of specimen shown in **c. e,** YKLP 11382b showing regions used in SEM-EDX mapping and fluorescence microscopy. **f,** close up of anterior region showing prostomial lobe and palp attachment. **g**, interpretative drawing of region shown in **f** showing major anatomical features, colour scheme as in Fig 1, and palp attachment inferred also with additional information from the counterpart. **h,** SEM-EDX elemental maps, element names for each map are shown in the bottom right corner. **i,** fluorescence image showing the anterior region of the body in YKLP 11382b including the gut, palps and putative blood lacuna. **j**, fluorescence image of putative blood lacuna in YKLP 11382a. **k,** close up of posterior fragment associated with the holotype with parapodial lamellae. Abbreviations: bl – blood lacuna, ch – chaetae, gu – gut, mo – mouth, pl – palps, plm – parapodial lamella, pro - prostomium.

Extended data Figure 2 | Specimen of *Dannychaeta tucolus* YKLP 11393 preserved in dwelling tube. a, YKLP 11393b specimen preserving anterior region, dwelling tube and a partial abdomen. **b**, YKLP 11393a specimen preserving anterior region, dwelling tubes and a partial abdomen. **c,** YKLP 11393b, close up of anterior region (boxed area shown in **a**), white arrowheads indicate the tube margins. **d,** interpretative drawing of region shown in **c. e** close up of prostomium and palps of c. **f,** YKLP 11393a, close up of anterior region (boxed area shown in **b**), white arrowheads indicate the tube margins. **g,** close up of same region as in **f,** using fluorescence microscope. **h,** interpretative drawing of region shown in **f** and **g. i,** poorly preserved abdominal region, from region shown in **a,** direct light. **j,** same region as in **i,** using fluorescence microscope. **k,** poorly preserved abdominal region, from region shown in **b,** direct light. **l,** same region as in **k,** using fluorescence microscope. **m,** thoracic chaetiger showing parapodia and chaetae from region shown in **b. n,** thoracic chaetiger showing parapodia and chaetae from region shown in **a.** Abbreviations: ch –chaetae, gu – gut, pa – parapodium, pro – prostomium, pl – palp.

Extended data Figure 3 | Additional details of specimen YKLP 11383, preserved inside dwelling tube parallel to bedding. a, YKLP 11383a midbody fragment preserved inside dwelling tube, part. **b,** interpretative drawing of specimen shown in **a,** regions demarcated by black and blue brackets represent decayed and well preserved regions of the body fossil, respectively. **c,** YKLP 11383b, midbody fragment preserved inside dwelling tube, counterpart. **d,** interpretative drawing of specimen shown in **c**. **e,** close up of well preserved region of YKLP 11383a in **a**, showing 11 chaetigers preserved inside the dwelling tube. **f,** SEM backscatter image of similar region to EDX maps shown in Figure 3f, showing bright grains associated with the tube and body fossil, arrowheads indicate the left tube margin and pyritised tube wall. **g,** section of fossil shown in **a** photographed under low angle light to indicate the relief of the dwelling tube. **h,** section of fossil shown in **c** photographed under low angle light to indicate the relief of the dwelling tube. **i,** close up of three chaetiger region of region shown in **e. j,** same region as in **i,** photographed using fluorescence microscope. **k,** close up of individual parapodium shown in **j**, photographed using fluorescence microscope. Abbreviations: ch – chaetae, gu – gut, pa – parapodium.

Extended data Figure 4 | Specimens YKLP 11384a, YKLP 11387 and YKLP 11401 showing effaced specimens preserved in dwelling tubes. a, YKLP 11384a, anterior fragment preserving thorax and abdomen preserved inside dwelling tube. **b,** YKLP 11387a, anterior fragment preserving thorax and abdomen. **c,** YKLP 11387b, anterior fragment preserving thorax and abdomen. **d,** close up of abdominal chaetigers in YKLP 11387a, from region shown in **b,** white filled arrows indicate the tube margins. **e,** same region as in **d** photographed using fluorescence microscope. **f,** YKLP 11401, effaced specimen preserved in dwelling tube preserving the putative blood lacuna. **g,** close up of region shown in **f,** showing gut and possible blood lacuna. Brackets on a, b, c and f indicate the position of the thoracic region. Abbreviations: bl – blood lacuna, ch – chaetae, gu – gut.

Extended data Figure 5 | Additional details of specimen YKLP 11389 showing details of parapodia, parapodial lamellae and the posterior region. a, YKLP 11389b, counterpart, posterior fragment preserving parapodia and chaetae. **b,** YKLP 11389a, part showing preservation of lateral parapodial lamellae. **c,** close up of five chaetigers from region shown in **a. d,** close up of chaetiger from region shown in **c**. **e,** close up of chaetiger in **d**. **f,** close up of chaetiger preserving parapodial lamellae from region shown in **b. g,** chaetigers preserving parapodial lamellae from region shown in **b. h,** same region as in **g** showing parapodial lamellae, photographed using fluorescence microscope. **i**, posterior region as shown in **a**, with putative pygidial cirri. **j,** close up of putative pygidial cirri in **i**. **k,** same region as in **j,** photographed with fluorescence microscope. Abbreviations: ch – chaetae, gu – gut, plm – parapodial lamella, pyc – pygidial cirri.

Extended data Figure 6 | Specimen YKLP 11384, a decayed specimen prerved in dwelling tube. a, YKLP 11384a, whole specimen in dwelling tube, white arrowheads indicate the tube margin. **b,** YKLP 11384b, whole specimen in dwelling tube, white arrowheads indicate the tube margin. **c,** details of YKLP 11384b, showing putative blood lacuna and gut, white and black arrowheads indicate the tube and body margins respectively. **d,** same view as in **c,** but imaged using fluorescence microscopy, note the thick appearance of the tube margin. **e,** detail of YKLP 11384a, showing preservation of the tube wall, indicated by white arrowheads.

Extended data Figure 7 | Full results of Bayesian phylogenetic analyses. a, full results of unconstrained analysis under the mki + gamma model, topology is a majority rule consensus tree and the scale bar is in units of expected number of substitutions per site, numbers at nodes are posterior probabilities. **b**, full results of analysis with constraints from phylogenomics under the mki + gamma model, topology is a majority rule consensus tree and the scale bar is in units of expected number of substitutions per site, numbers at nodes are posterior probabilities.

Extended data Figure 8 | Results of parsimony analyses under equal and implied weighting. a, Strict consensus tree (length 1071) of parsimony analysis without topological constraints, numbers at nodes are support from bootstrapping, jacknifing and Bremer decay. **b,** strict consensus of trees inferred using implied weighting at k=10 (tree score 46.14190), numbers at nodes are relative frequencies from symmetric resampling.

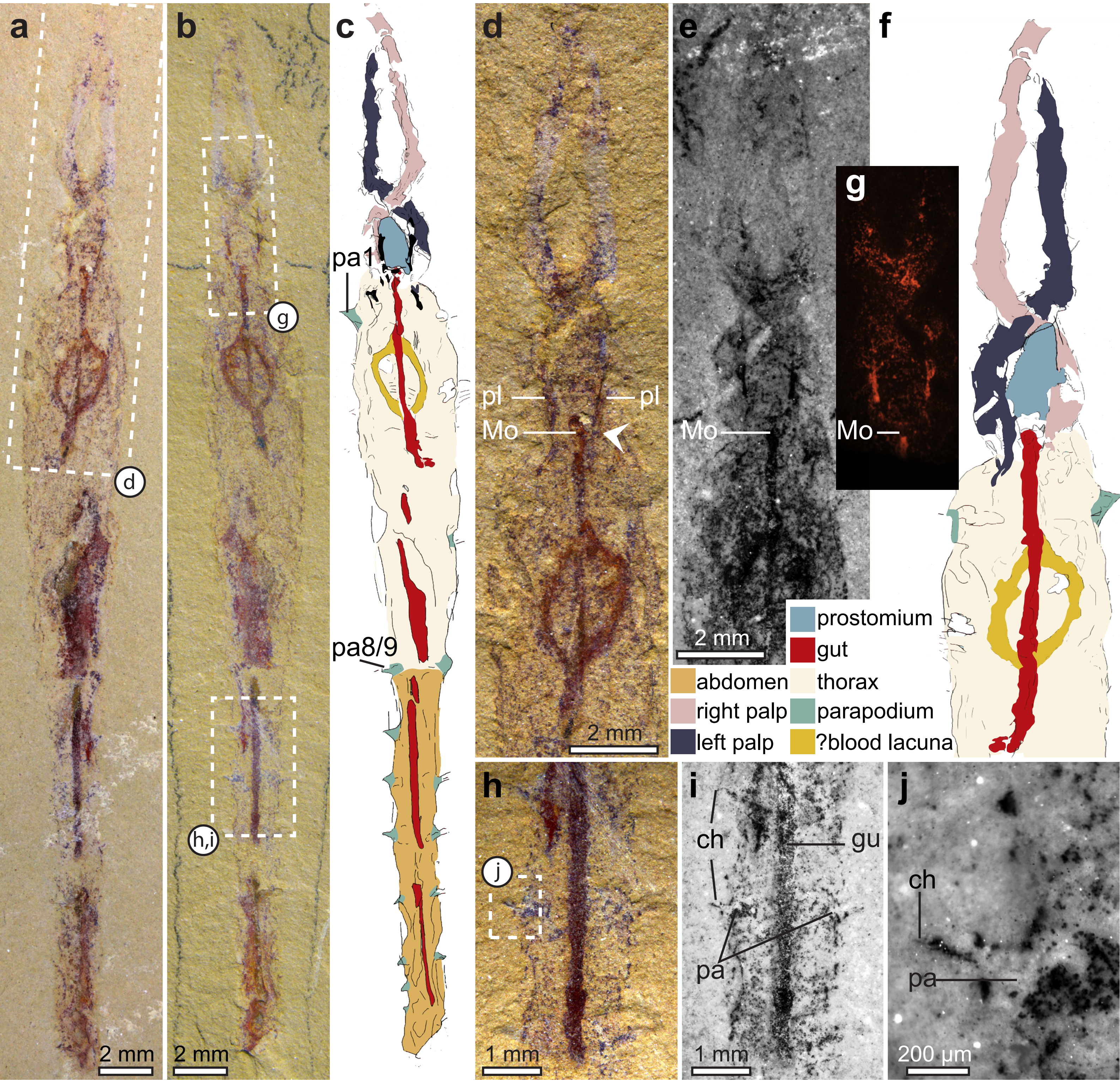
a
b
c
d
e
f
g
h
i
j
d
g
h,i
j
pa1
pa8/9
pl
pl
Mo
Mo
Mo
ch
gu
ch
pa
pa
prostomium
gut
abdomen
thorax
right palp
parapodium
left palp
?blood lacuna
2 mm
2 mm
2 mm
2 mm
1 mm
1 mm
200 µm

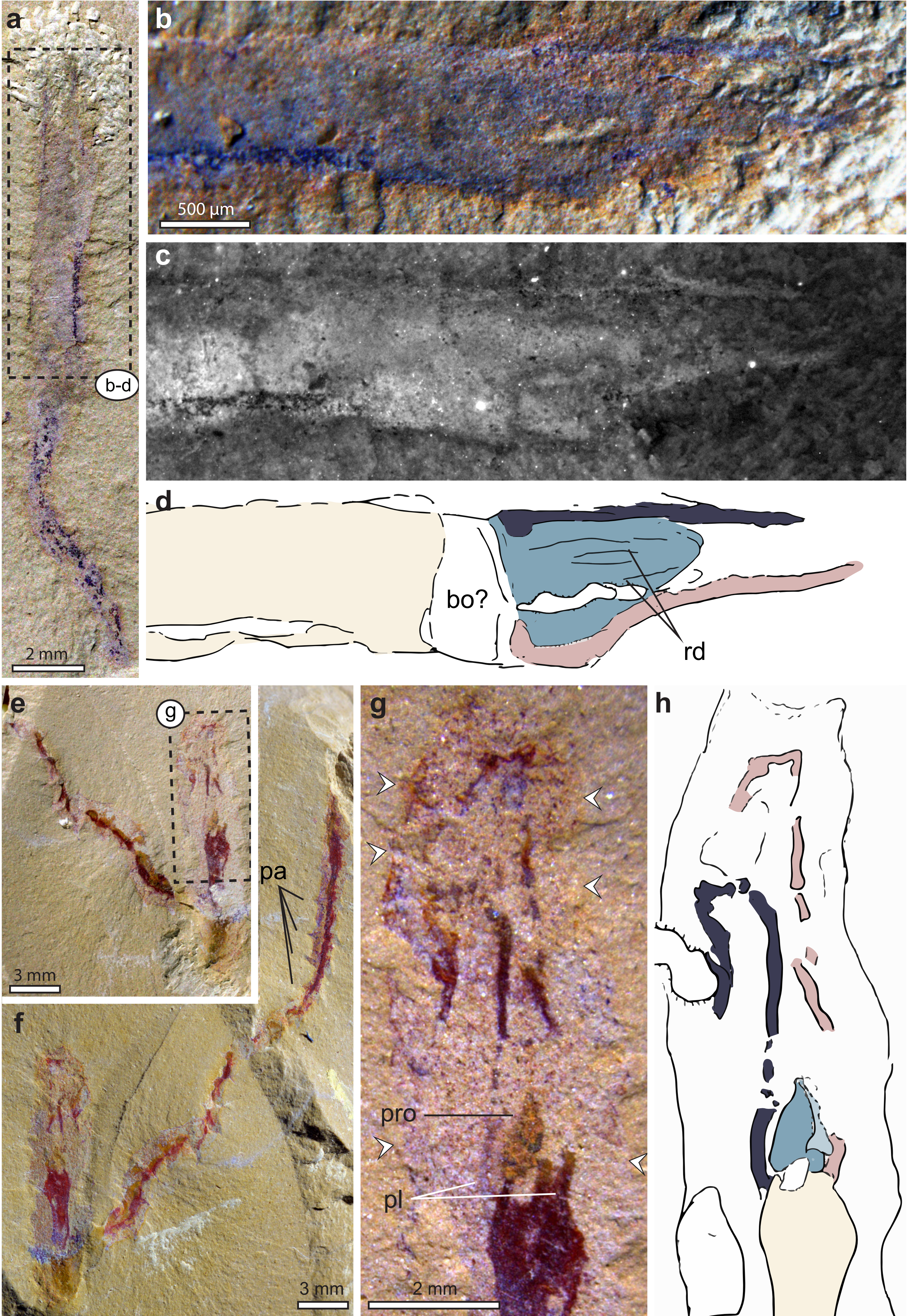
a
b-d
2 mm
b
500 µm
c
d
bo?
rd
e
g
pa
3 mm
f
3 mm
g
pro
pl
2 mm
h

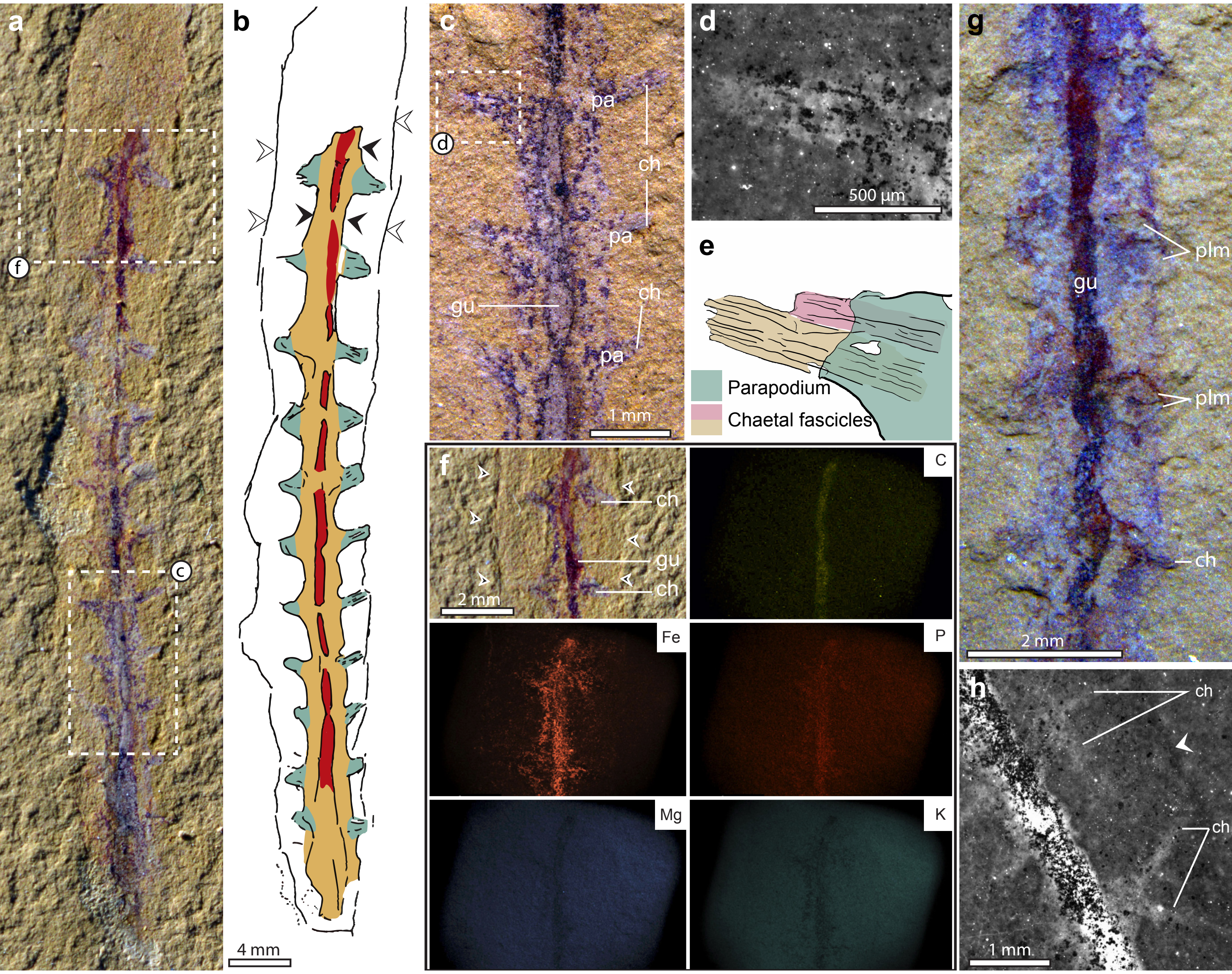

a
f
c
b
4 mm
c
d
pa
ch
pa
gu
ch
pa
1 mm
d
500 µm
e
Parapodium
Chaetal fascicles
f
ch
gu
ch
2 mm
C
Fe
P
Mg
K
g
plm
gu
plm
ch
2 mm
h
ch
ch
1 mm

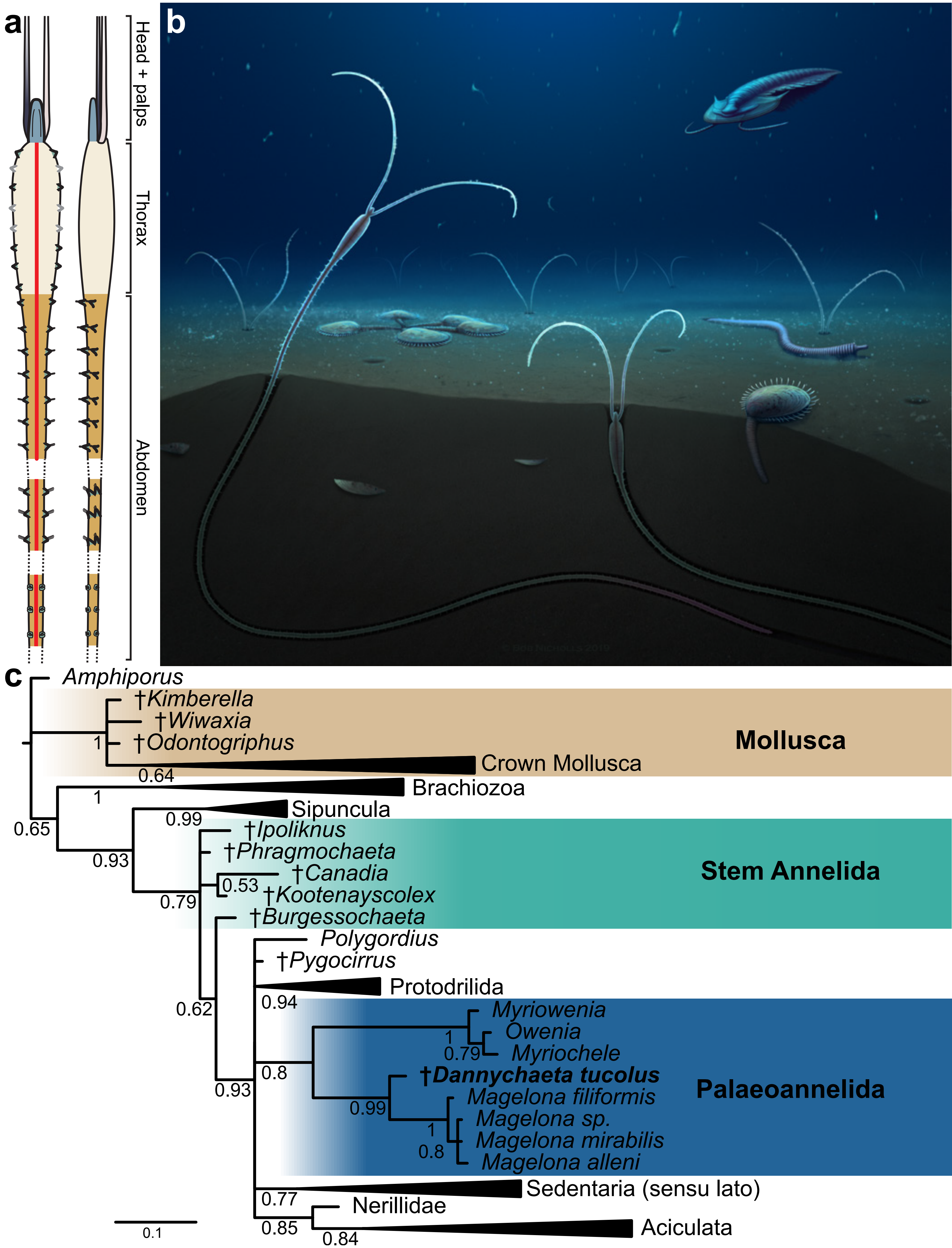
a
Head + palps
Thorax
Abdomen
b
© Bob Nicholls 2019
c
Amphiporus
†Kimberella
†Wiwaxia
1
†Odontogriphus
Mollusca
Crown Mollusca
0.64
Brachiozoa
1
0.65
Sipuncula
0.99
0.93
†Ipoliknus
†Phragmochaeta
†Canadia
0.53
†Kootenayscolex
0.79
†Burgessochaeta
Stem Annelida
Polygordius
†Pygocirrus
Protodrilida
0.94
0.62
Myriowenia
1
Owenia
0.79
Myriochele
0.8
†Dannychaeta tucolus
Magelona filiformis
0.99
1
Magelona sp.
Magelona mirabilis
0.8
Magelona alleni
0.93
Palaeoannelida
Sedentaria (sensu lato)
0.77
Nerillidae
0.85
Aciculata
0.84
0.1

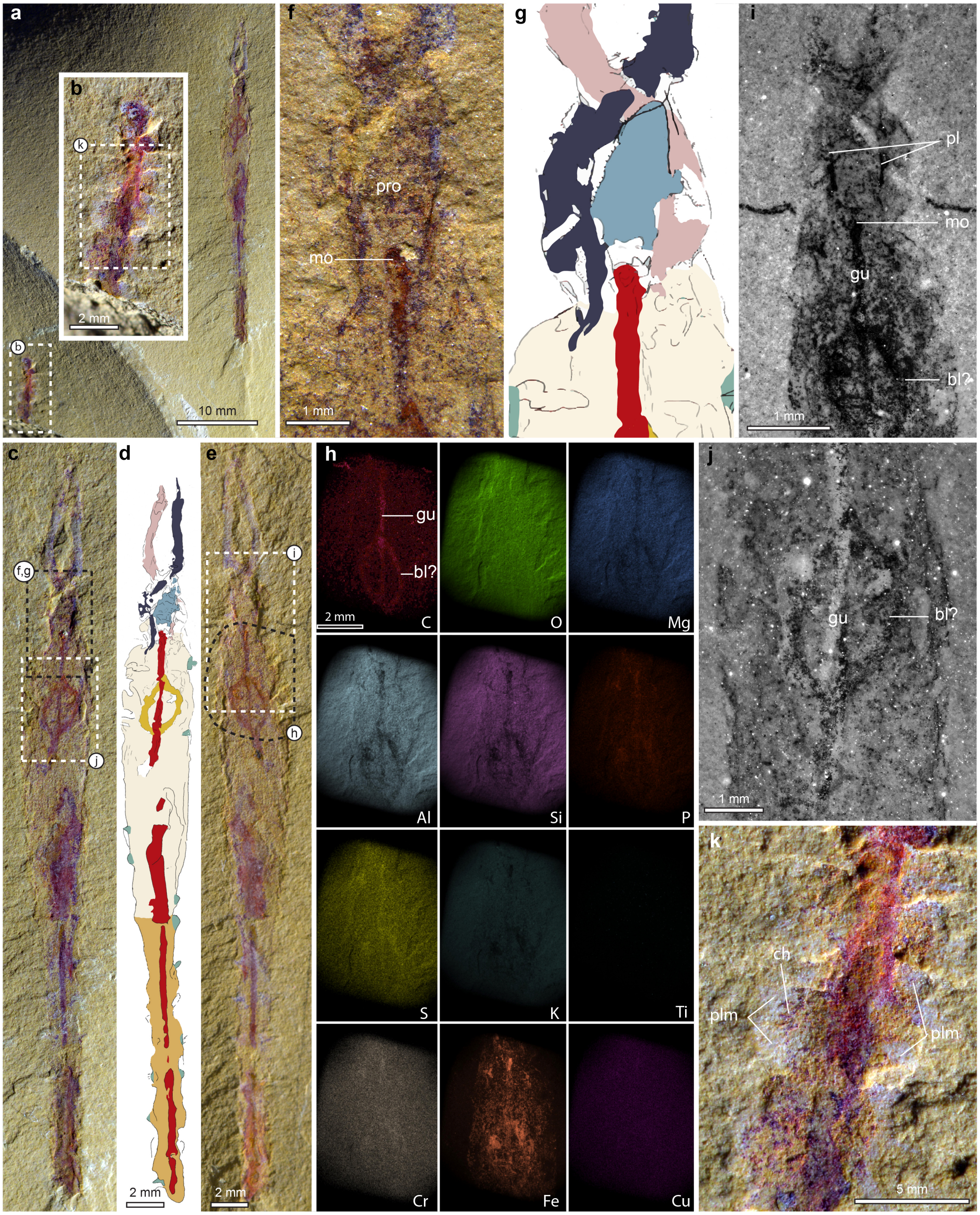
a
b
k
2 mm
b
10 mm
f
pro
mo
1 mm
g
i
pl
mo
gu
bl?
1 mm
c
f,g
j
d
2 mm
e
i
h
2 mm
h
gu
bl?
2 mm
C
O
Mg
Al
Si
P
S
K
Ti
Cr
Fe
Cu
j
gu
bl?
1 mm
k
ch
plm
plm
5 mm

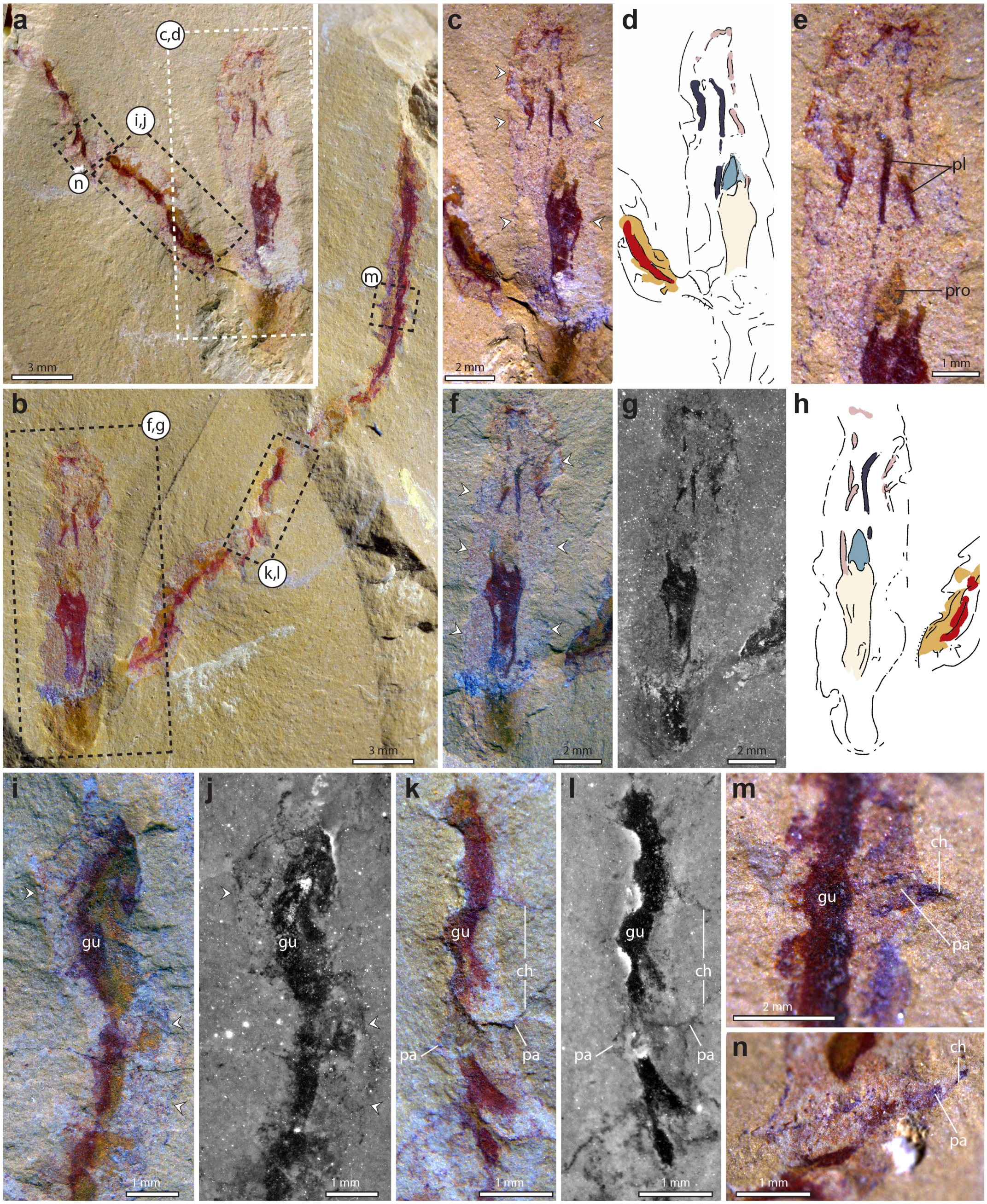
a
c,d
i,j
n
m
3 mm
b
f,g
k,l
3 mm
c
2 mm
d
e
pl
pro
1 mm
f
2 mm
g
2 mm
h
i
gu
1 mm
j
gu
1 mm
k
gu
ch
pa
pa
1 mm
l
gu
ch
pa
pa
1 mm
m
ch
gu
pa
2 mm
n
ch
pa
1 mm

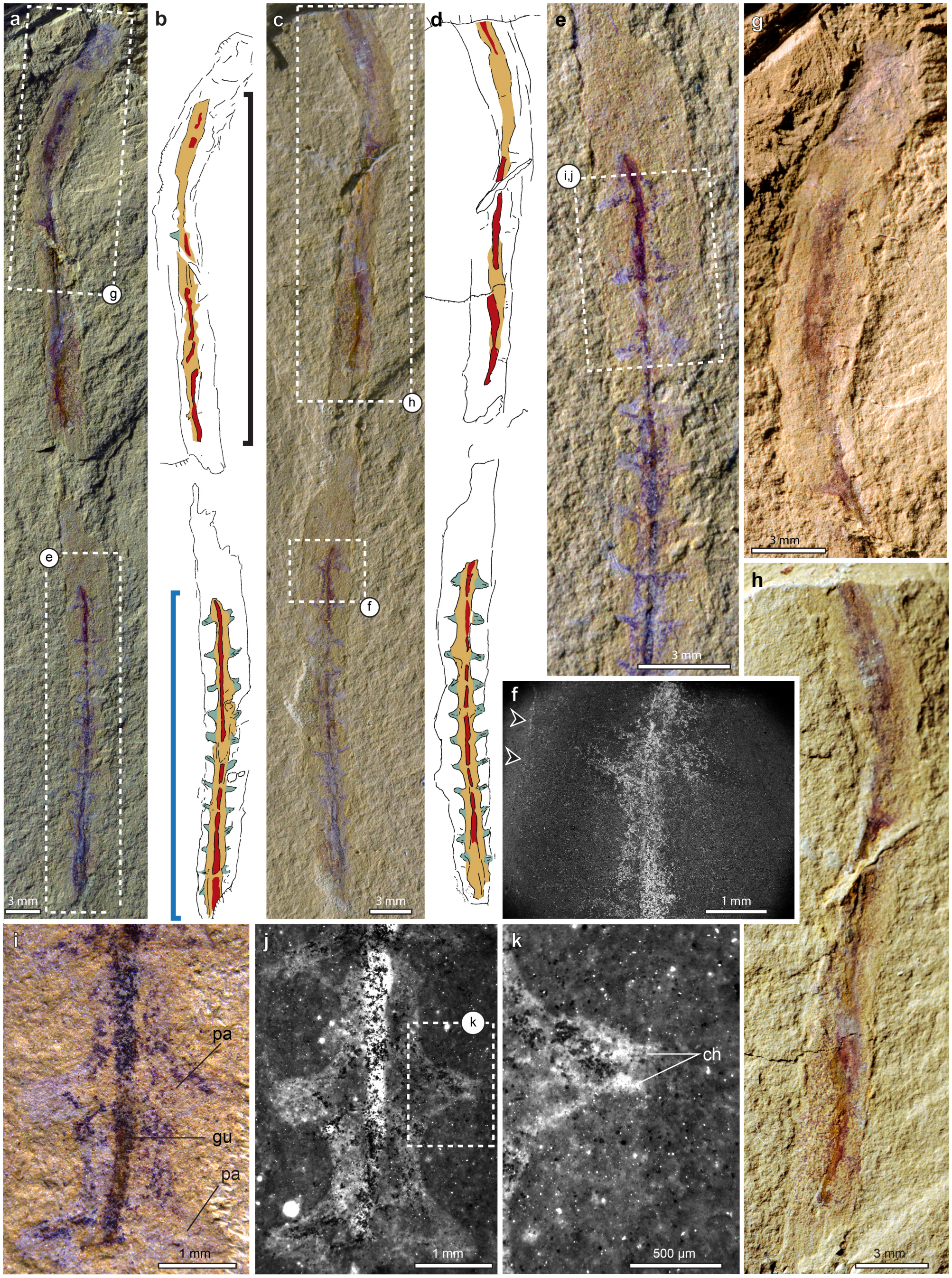
a
g
e
3 mm
b
c
h
f
3 mm
d
e
i,j
3 mm
f
1 mm
g
3 mm
h
3 mm
i
pa
gu
pa
1 mm
j
k
1 mm
k
ch
500 µm

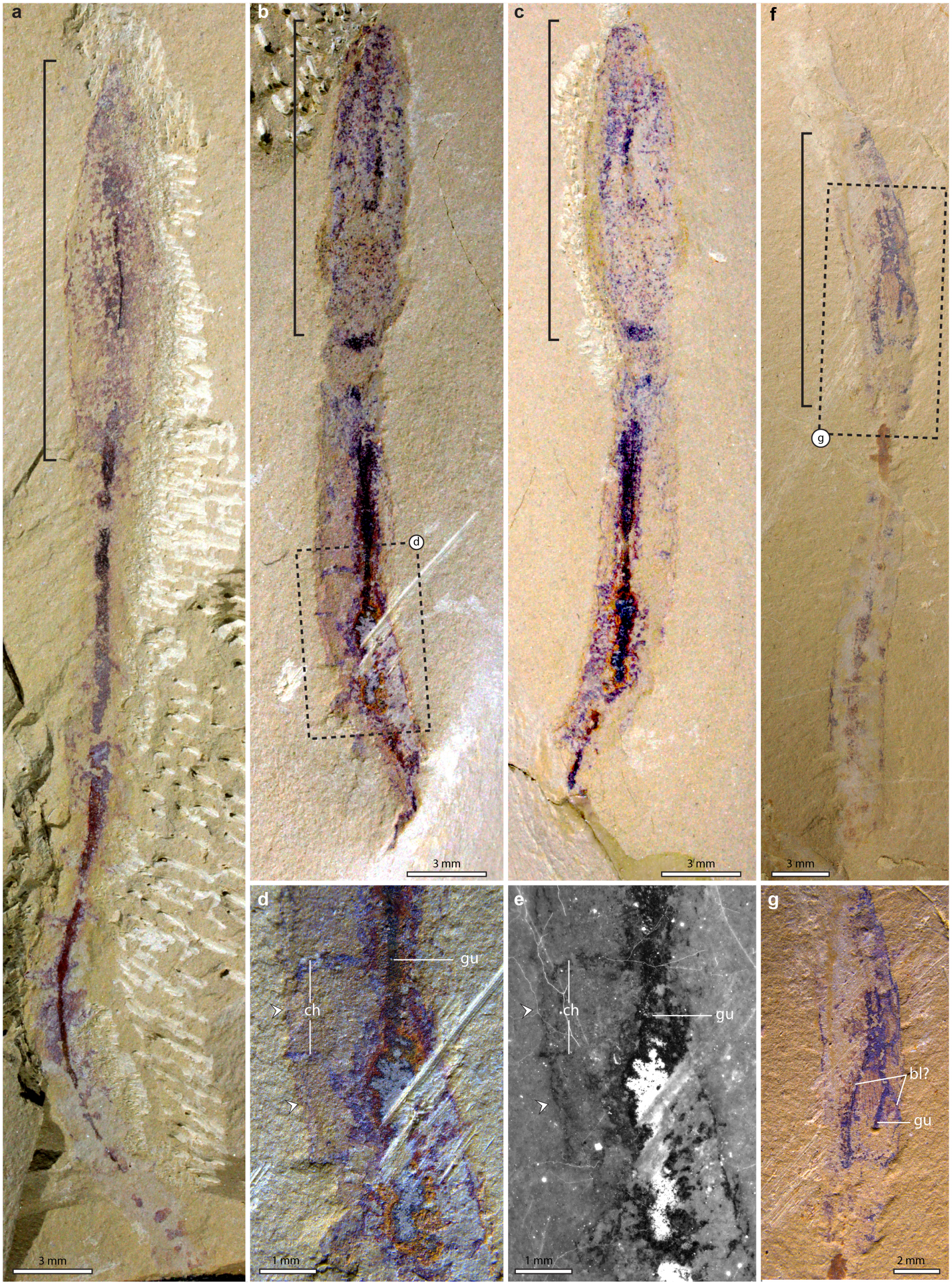
a
3 mm
b
d
3 mm
c
3 mm
f
g
3 mm
d
gu
ch
1 mm
e
ch
gu
1 mm
g
bl?
gu
2 mm

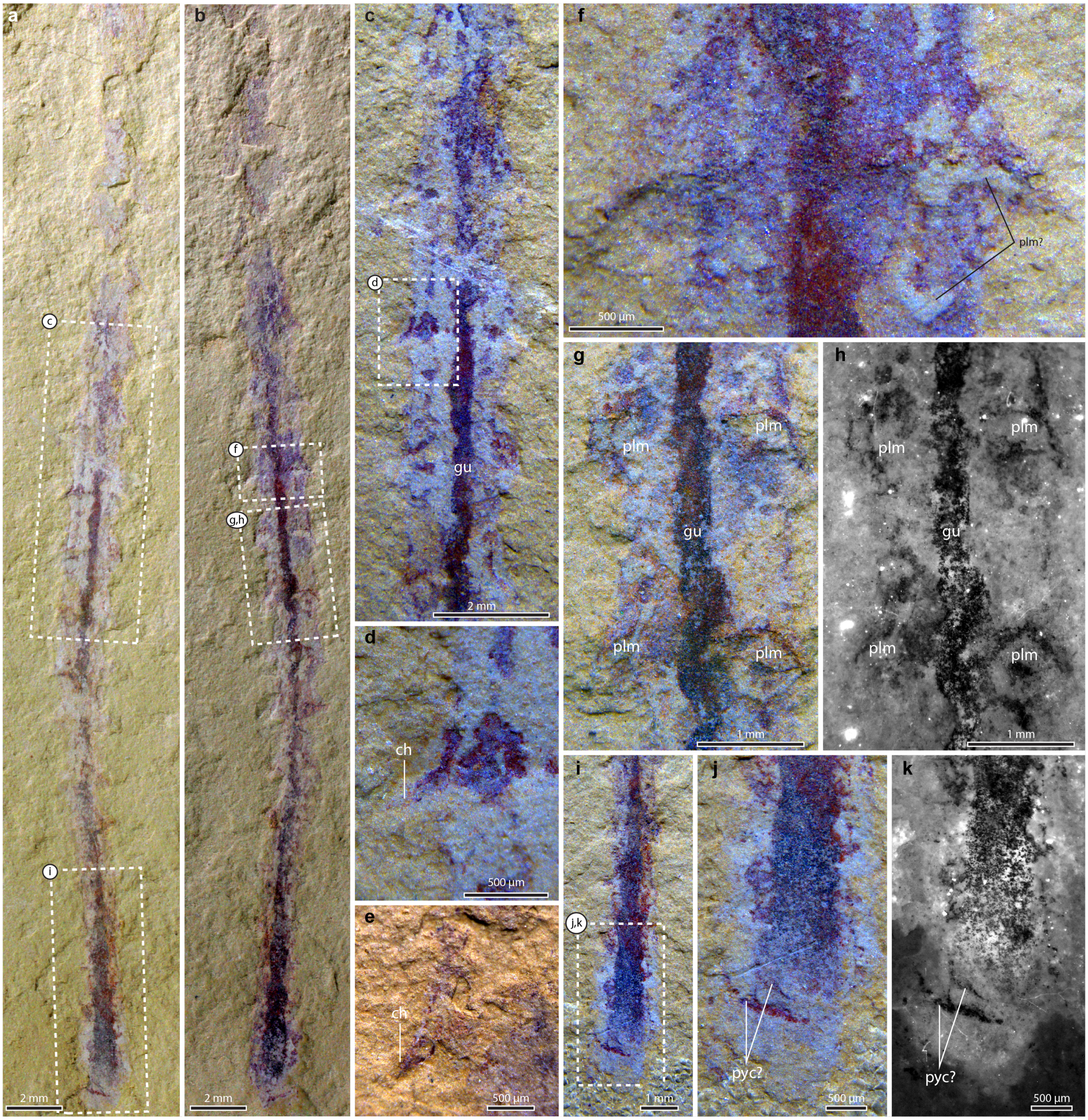
a
c
i
2 mm
b
f
g,h
2 mm
c
d
gu
2 mm
d
ch
500 µm
e
ch
500 µm
f
plm?
500 µm
g
plm
plm
gu
plm
plm
1 mm
h
plm
plm
gu
plm
plm
1 mm
i
j,k
1 mm
j
pyc?
500 µm
k
pyc?
500 µm

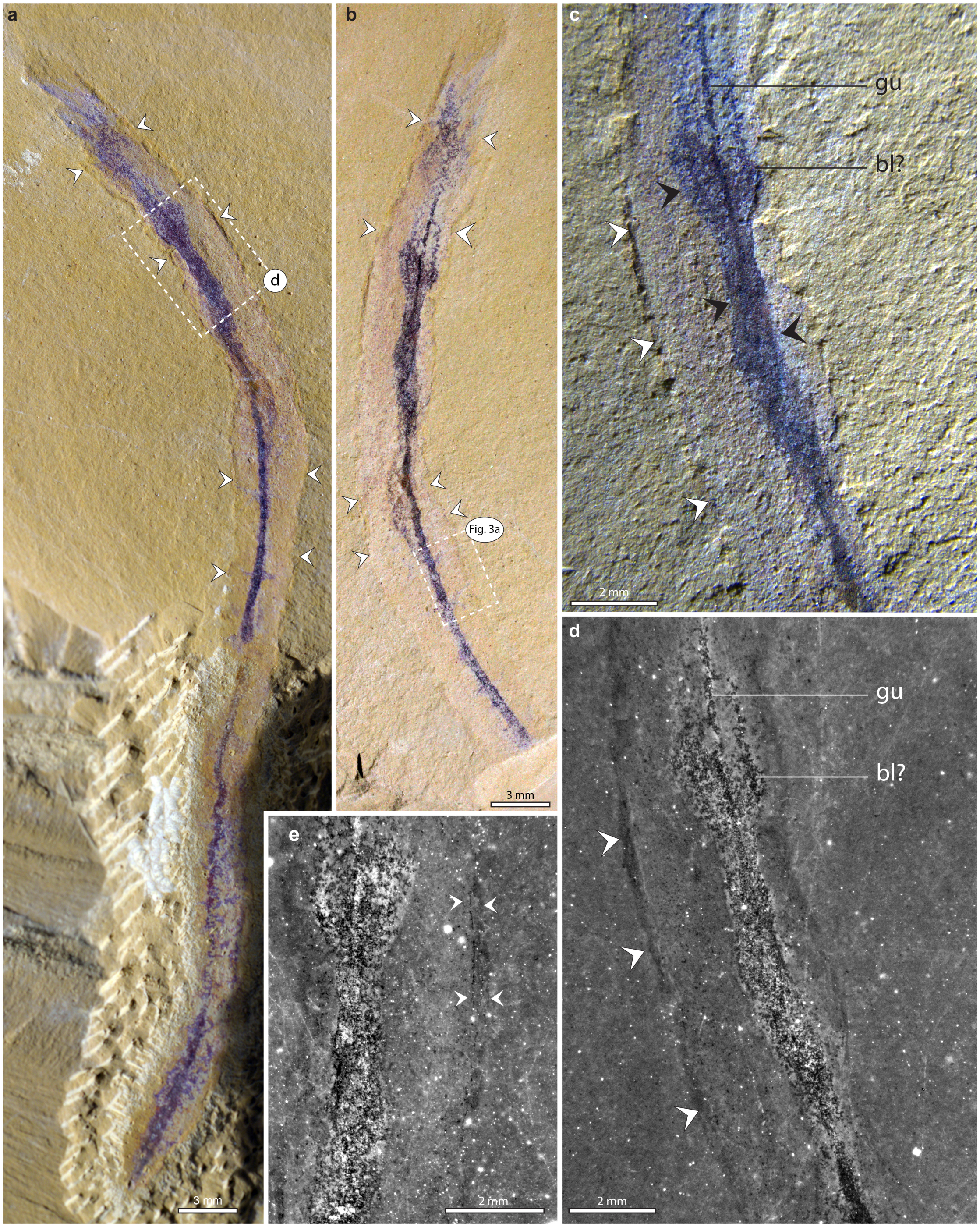
a
d
3 mm
b
Fig. 3a
3 mm
c
gu
bl?
2 mm
d
gu
bl?
2 mm
e
2 mm

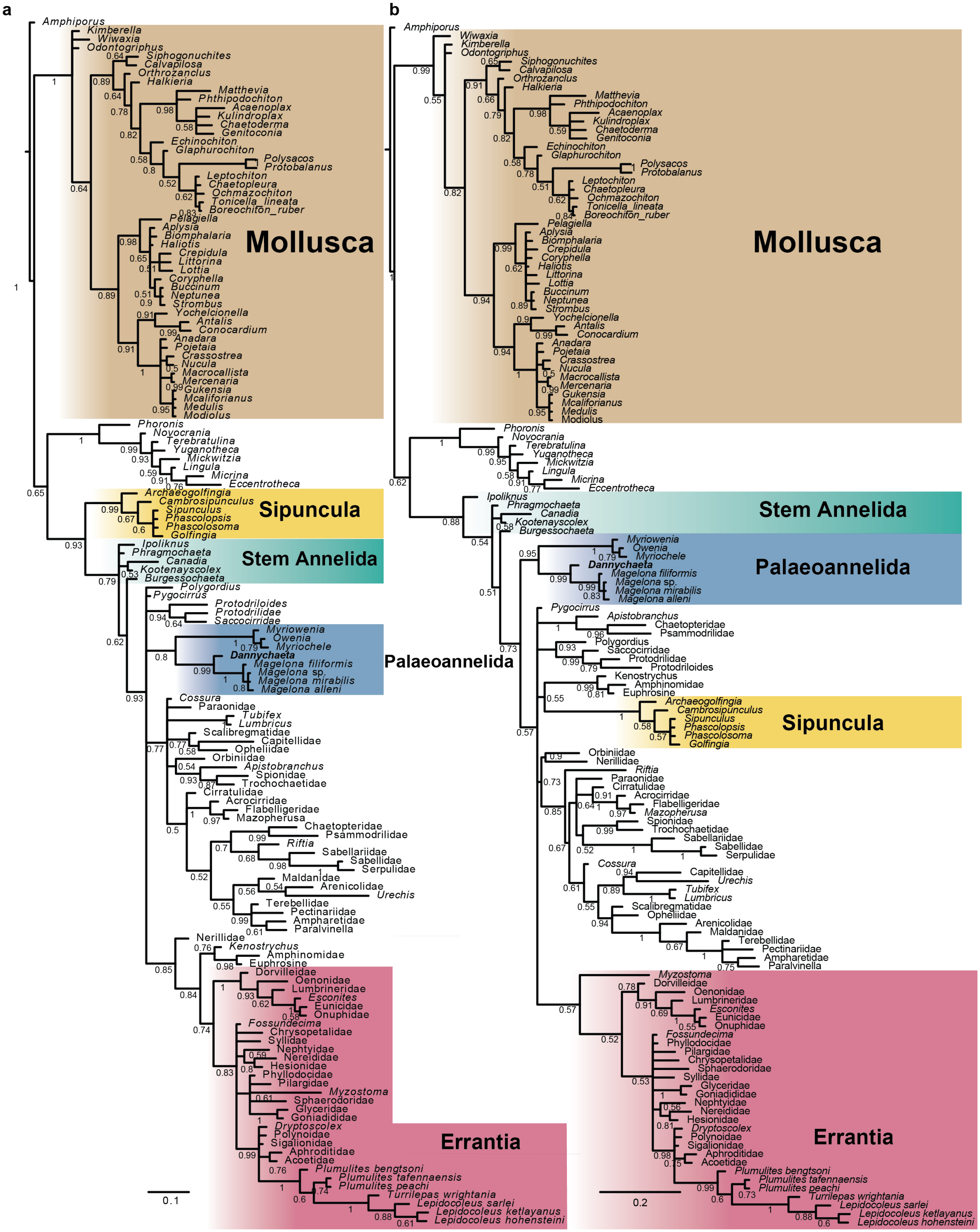
a
Amphiporus
Kimberella
Wiwaxia
Odontogriphus
Siphogonuchites
Calvapilosa
Orthrozanclus
Halkieria
Matthevia
Phthipodochiton
Acaenoplax
Kulindroplax
Chaetoderma
Genitoconia
Echinochiton
Glaphurochiton
Polysacos
Protobalanus
Leptochiton
Chaetopleura
Ochmazochiton
Tonicella_lineata
Boreochiton_ruber
Pelagiella
Aplysia
Biomphalaria
Haliotis
Crepidula
Littorina
Lottia
Coryphella
Buccinum
Neptunea
Strombus
Yochelcionella
Antalis
Conocardium
Anadara
Pojetaia
Crassostrea
Nucula
Macrocallista
Mercenaria
Gukensia
Mcaliforianus
Medulis
Modiolus
Mollusca
Phoronis
Novocrania
Terebratulina
Yuganotheca
Mickwitzia
Lingula
Micrina
Eccentrotheca
Archaeogolfingia
Cambrosipunculus
Sipunculus
Phascolopsis
Phascolosoma
Golfingia
Sipuncula
Ipoliknus
Phragmochaeta
Canadia
Kootenayscolex
Burgessochaeta
Stem Annelida
Polygordius
Pygocirrus
Protodriloides
Protodrilidae
Saccocirridae
Myriowenia
Owenia
Myriochele
Dannychaeta
Magelona filiformis
Magelona sp.
Magelona mirabilis
Magelona alleni
Palaeoannelida
Cossura
Paraonidae
Tubifex
Lumbricus
Scalibregmatidae
Capitellidae
Opheliidae
Orbiniidae
Apistobranchus
Spionidae
Trochochaetidae
Cirratulidae
Acrocirridae
Flabelligeridae
Mazopherusa
Chaetopteridae
Psammodrilidae
Riftia
Sabellariidae
Sabellidae
Serpulidae
Maldanidae
Arenicolidae
Urechis
Terebellidae
Pectinariidae
Ampharetidae
Paralvinella
Nerillidae
Kenostrychus
Amphinomidae
Euphrosine
Dorvilleidae
Oenonidae
Lumbrineridae
Esconites
Eunicidae
Onuphidae
Fossundecima
Chrysopetalidae
Syllidae
Nephtyidae
Nereididae
Hesionidae
Phyllodocidae
Pilargidae
Myzostoma
Sphaerodoridae
Glyceridae
Goniadidae
Dryptoscolex
Polynoidae
Sigalionidae
Aphroditidae
Acoetidae
Plumulites bengtsoni
Plumulites tafennaensis
Plumulites peachi
Turrilepas wrightania
Lepidocoleus sarlei
Lepidocoleus ketlayanus
Lepidocoleus hohensteini
Errantia
0.1
b
Amphiporus
Wiwaxia
Kimberella
Odontogriphus
Siphogonuchites
Calvapilosa
Orthrozanclus
Halkieria
Matthevia
Phthipodochiton
Acaenoplax
Kulindroplax
Chaetoderma
Genitoconia
Echinochiton
Glaphurochiton
Polysacos
Protobalanus
Leptochiton
Chaetopleura
Ochmazochiton
Tonicella_lineata
Boreochiton_ruber
Pelagiella
Aplysia
Biomphalaria
Crepidula
Coryphella
Haliotis
Littorina
Lottia
Buccinum
Neptunea
Strombus
Yochelcionella
Antalis
Conocardium
Anadara
Pojetaia
Crassostrea
Nucula
Macrocallista
Mercenaria
Gukensia
Mcaliforianus
Medulis
Modiolus
Mollusca
Phoronis
Novocrania
Terebratulina
Yuganotheca
Mickwitzia
Lingula
Micrina
Eccentrotheca
Ipoliknus
Phragmochaeta
Canadia
Kootenayscolex
Burgessochaeta
Stem Annelida
Myriowenia
Owenia
Myriochele
Dannychaeta
Magelona filiformis
Magelona sp.
Magelona mirabilis
Magelona alleni
Palaeoannelida
Pygocirrus
Apistobranchus
Chaetopteridae
Psammodrilidae
Polygordius
Saccocirridae
Protodrilidae
Protodriloides
Kenostrychus
Amphinomidae
Euphrosine
Archaeogolfingia
Cambrosipunculus
Sipunculus
Phascolopsis
Phascolosoma
Golfingia
Sipuncula
Orbiniidae
Nerillidae
Riftia
Paraonidae
Cirratulidae
Acrocirridae
Flabelligeridae
Mazopherusa
Spionidae
Trochochaetidae
Sabellariidae
Sabellidae
Serpulidae
Cossura
Capitellidae
Urechis
Tubifex
Lumbricus
Scalibregmatidae
Opheliidae
Arenicolidae
Maldanidae
Terebellidae
Pectinariidae
Ampharetidae
Paralvinella
Myzostoma
Dorvilleidae
Oenonidae
Lumbrineridae
Esconites
Eunicidae
Onuphidae
Fossundecima
Phyllodocidae
Pilargidae
Chrysopetalidae
Sphaerodoridae
Syllidae
Glyceridae
Goniadidae
Nephtyidae
Nereididae
Hesionidae
Dryptoscolex
Polynoidae
Sigalionidae
Aphroditidae
Acoetidae
Plumulites bengtsoni
Plumulites tafennaensis
Plumulites peachi
Turrilepas wrightania
Lepidocoleus sarlei
Lepidocoleus ketlayanus
Lepidocoleus hohensteini
Errantia
0.2

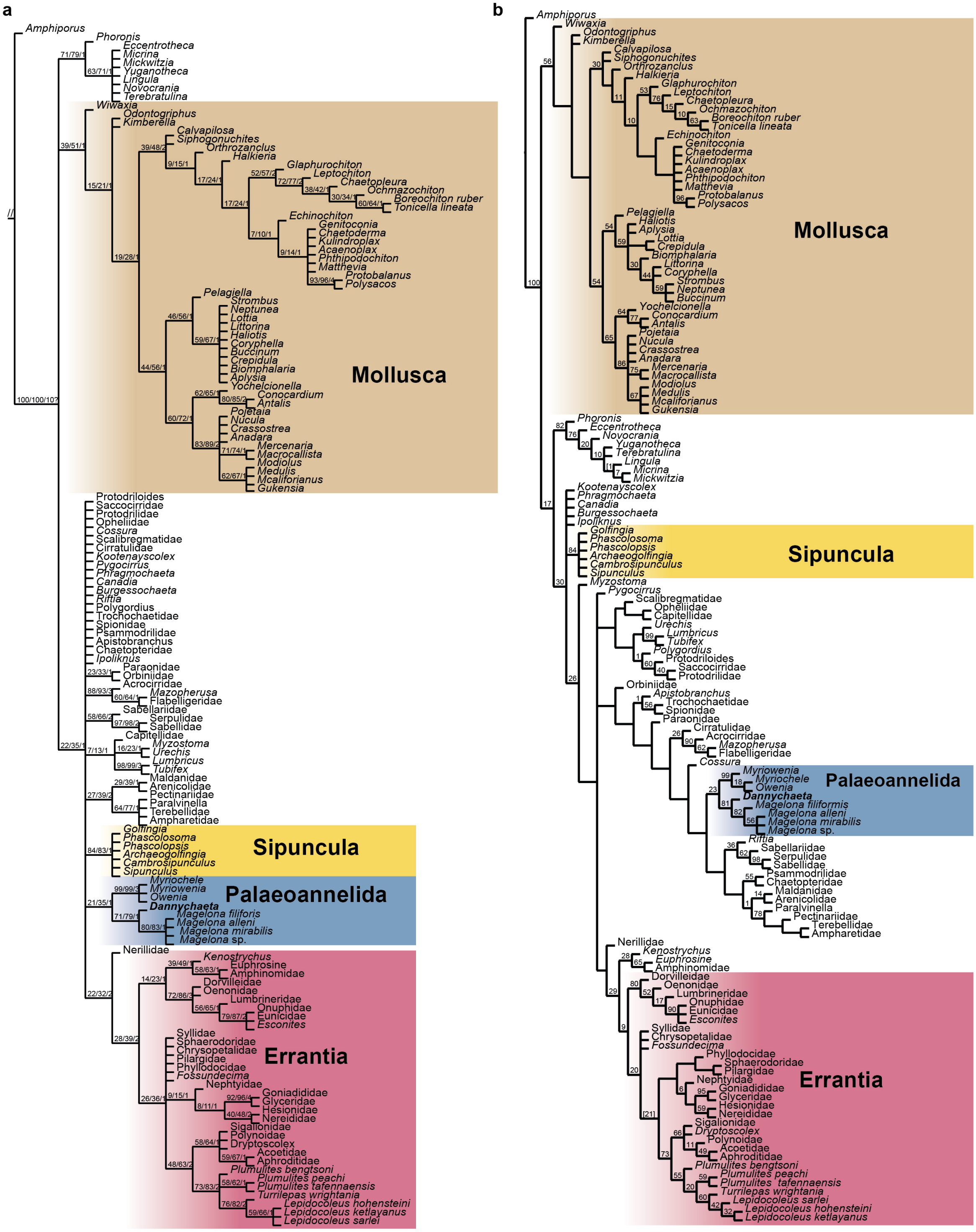
a
Amphiporus
Phoronis
Eccentrotheca
Micrina
Mickwitzia
Yuganotheca
Lingula
Novocrania
Terebratulina
71/79/1
63/71/1
Wiwaxia
Odontogriphus
Kimberella
Calvapilosa
Siphogonuchites
Orthrozanclus
Halkieria
Glaphurochiton
Leptochiton
Chaetopleura
Ochmazochiton
Boreochiton ruber
Tonicella lineata
Echinochiton
Genitoconia
Chaetoderma
Kulindroplax
Acaenoplax
Phthipodochiton
Matthevia
Protobalanus
Polysacos
39/51/1
15/21/1
39/48/2
9/15/1
17/24/1
52/57/2
72/77/2
38/42/1
30/34/1
60/64/1
17/24/1
7/10/1
9/14/1
93/96/4
19/28/1
Pelagiella
Strombus
Neptunea
Lottia
Littorina
Haliotis
Coryphella
Buccinum
Crepidula
Biomphalaria
Aplysia
Yochelcionella
Conocardium
Antalis
Pojetaia
Nucula
Crassostrea
Anadara
Mercenaria
Macrocallista
Modiolus
Medulis
Mcaliforianus
Gukensia
46/56/1
59/67/1
44/56/1
62/65/1
80/85/2
60/72/1
83/89/2
71/74/1
62/67/1
Mollusca
//
100/100/10?
Protodriloides
Saccocirridae
Protodrilidae
Opheliidae
Cossura
Scalibregmatidae
Cirratulidae
Kootenayscolex
Pygocirrus
Phragmochaeta
Canadia
Burgessochaeta
Riftia
Polygordius
Trochochaetidae
Spionidae
Psammodrilidae
Apistobranchus
Chaetopteridae
Ipoliknus
Paraonidae
Orbiniidae
Acrocirridae
Mazopherusa
Flabelligeridae
Sabellariidae
Serpulidae
Sabellidae
Capitellidae
Myzostoma
Urechis
Lumbricus
Tubifex
Maldanidae
Arenicolidae
Pectinariidae
Paralvinella
Terebellidae
Ampharetidae
23/33/1
88/93/3
60/64/1
58/66/2
97/98/2
22/35/1
7/13/1
16/23/1
98/99/3
27/39/2
29/39/1
64/77/1
Golfingia
Phascolosoma
Phascolopsis
Archaeogolfingia
Cambrosipunculus
Sipunculus
84/83/1
Sipuncula
Myriochele
Myriowenia
Owenia
Dannychaeta
Magelona filiforis
Magelona alleni
Magelona mirabilis
Magelona sp.
21/35/1
99/99/3
71/79/1
80/83/1
Palaeoannelida
Nerillidae
Kenostrychus
Euphrosine
Amphinomidae
Dorvilleidae
Oenonidae
Lumbrineridae
Onuphidae
Eunicidae
Esconites
22/32/2
14/23/1
39/49/1
58/63/1
72/86/3
56/65/1
79/87/2
28/39/2
Syllidae
Sphaerodoridae
Chrysopetalidae
Pilargidae
Phyllodocidae
Fossundecima
Nephtyidae
Goniadididae
Glyceridae
Hesionidae
Nereididae
Sigalionidae
Polynoidae
Dryptoscolex
Acoetidae
Aphroditidae
Plumulites bengtsoni
Plumulites peachi
Plumulites tafennaensis
Turrilepas wrightania
Lepidocoleus hohensteini
Lepidocoleus ketlayanus
Lepidocoleus sarlei
26/36/1
9/15/1
8/11/1
92/96/4
40/48/2
58/64/1
59/67/1
48/63/2
73/83/2
58/62/1
76/82/2
59/66/1
Errantia
b
Amphiporus
Wiwaxia
Odontogriphus
Kimberella
Calvapilosa
Siphogonuchites
Orthrozanclus
Halkieria
Glaphurochiton
Leptochiton
Chaetopleura
Ochmazochiton
Boreochiton ruber
Tonicella lineata
Echinochiton
Genitoconia
Chaetoderma
Kulindroplax
Acaenoplax
Phthipodochiton
Matthevia
Protobalanus
Polysacos
56
30
11
53
76
15
10
63
10
96
100
Pelagiella
Haliotis
Aplysia
Lottia
Crepidula
Biomphalaria
Littorina
Coryphella
Strombus
Neptunea
Buccinum
Yochelcionella
Conocardium
Antalis
Pojetaia
Nucula
Crassostrea
Anadara
Mercenaria
Macrocallista
Modiolus
Medulis
Mcaliforianus
Gukensia
54
59
30
44
59
54
64
77
65
86
75
67
Mollusca
Phoronis
Eccentrotheca
Novocrania
Yuganotheca
Terebratulina
Lingula
Micrina
Mickwitzia
82
76
20
10
11
7
17
Kootenayscolex
Phragmochaeta
Canadia
Burgessochaeta
Ipoliknus
Golfingia
Phascolosoma
Phascolopsis
Archaeogolfingia
Cambrosipunculus
Sipunculus
84
Sipuncula
Myzostoma
30
Pygocirrus
Scalibregmatidae
Opheliidae
Capitellidae
Urechis
Lumbricus
Tubifex
Polygordius
Protodriloides
Saccocirridae
Protodrilidae
99
1
60
40
26
Orbiniidae
Apistobranchus
Trochochaetidae
Spionidae
Paraonidae
Cirratulidae
Acrocirridae
Mazopherusa
Flabelligeridae
Cossura
1
56
26
90
62
Myriowenia
Myriochele
Owenia
Dannychaeta
Magelona filiformis
Magelona alleni
Magelona mirabilis
Magelona sp.
99
18
23
81
82
56
Palaeoannelida
Riftia
Sabellariidae
Serpulidae
Sabellidae
Psammodrilidae
Chaetopteridae
Maldanidae
Arenicolidae
Paralvinella
Pectinariidae
Terebellidae
Ampharetidae
36
62
98
55
14
1
78
Nerillidae
Kenostrychus
Euphrosine
Amphinomidae
Dorvilleidae
Oenonidae
Lumbrineridae
Onuphidae
Eunicidae
Esconites
28
65
29
80
52
17
90
9
Syllidae
Chrysopetalidae
Fossundecima
Phyllodocidae
Sphaerodoridae
Pilargidae
Nephtyidae
Goniadididae
Glyceridae
Hesionidae
Nereididae
Sigalionidae
Dryptoscolex
Polynoidae
Acoetidae
Aphroditidae
Plumulites bengtsoni
Plumulites peachi
Plumulites tafennaensis
Turrilepas wrightania
Lepidocoleus sarlei
Lepidocoleus hohensteini
Lepidocoleus ketlayanus
20
[21]
6
95
59
66
11
49
73
55
59
20
60
42
32
Errantia